research articles Journal of proteome research

Proteomics Analysis Reveals Insight into the Mechanism of H-Ras-Mediated Transformation

Bao-Feng Jin,§ Kun He,§ Hong-Xia Wang, Bing Bai, Tao Zhou, Hui-Yan Li, Jiang-Hong Man, Bing-Yu Liu, Wei-Li Gong, Jie Wang, Ai-Ling Li,* and Xue-Min Zhang*

Institute of Basic Medical Sciences, National Center of Biomedical Analysis, Beijing 100850, China

Received June 11, 2006

We implemented a proteomics approach to the systematical analysis of the alterations in the proteome of NIH3T3 cells transformed by oncogenic H-RasV12. Forty-four proteins associated with Ras-mediated transformation have been identified, and 28 proteins were not previously reported. RT-PCR analysis showed that approximately 44% of target proteins identified showed concomitant changes in mRNA abundance. A principal finding was the up-regulation of gankyrin, which was the first evidence to show that gankyrin pathway was implicated in Ras-activated transformation.

Keywords: Oncogenic Ras • Transformation • Proteomics • Gankyrin

Introduction

Ras is a small GTP binding protein mutated in approximately 30% of human cancer, initially identified by virtue of their oncogenic potential, and has long been known to play a significant role in tumor formation and development.[1−3] Overexpression of activated Ras leads to tumorigenesis in transgenic mice and in naturally occurring human neoplasia.[4−6] In addition, Ras function as regulated GDP/GTP molecular switches that control diverse signaling networks and are involved in a number of biological processes including growth, differentiation, proliferation, survival, cytoskeletal changes, and so on.[7] Ras activation occurs by recruitment to the membrane, followed by recognition of specific tyrosine phosphorylated sites in growth factor receptors.[1] The nature of the downstream targets of Ras has only recently begun to be elucidated, including c-Jun, Raf, Ral-GDS, p110, RGL, Tiam1, PLC ϵ, AF-6, RasIP1, RasSF, IMP, and others, which serve as regulators and effectors, as well as signaling integrators, of Ras signaling.[7] Activation of H-Ras upstream and downstream effector pathways is often demonstrated in the absence of H-Ras mutation. For example, the downstream signaling molecule Raf-1 exhibits the same transforming potency as oncogenic Ras, and Raf-1 activation alone is sufficient to mediate full Ras transforming activity.[8] Despite the evidence that Raf-1 is a critical downstream effector of Ras function, there is increasing evidence that Ras may mediate its actions through the activation of multiple downstream effector-mediated pathways.[9] The recent identification of other candidate Ras effectors (e.g., RalGDS and PI-3 kinase) suggests that activation of other downstream effector-mediated signaling pathways may also mediate Ras transforming activity.[8] These pathways can act independently, or synergistically, to cause cellular transformation. It is important to resolve what these pathways are and to establish their contributions to tumorigenicity.

Although multiple mediators of Ras signaling have been discovered, the exact mechanism by which oncogenic Ras acts in the multistep process of oncogenesis is not completely understood, and many downstream functions of Ras signaling in cellular transformation remain a mystery.[3] The molecular mechanism of Ras-mediated oncogenic transformation as a whole has been detected by cDNA expression array.[10] Nevertheless, it should be stressed that mRNA levels do not necessarily correlate with protein levels.[11] Recently, technological advances in proteomics allow us to examine the expression profiles at the protein level on a genomewide scale. During our research on the proteomics analysis, we noticed a recent report on proteomics analysis of H-Ras-mediated transformation in human ovarian cancer model.[3] However, our proteomics analysis revealed different alterations in the cellular proteome of NIH3T3 cells transformed by H-Ras. Moreover, our study identified gankyrin as a novel protein targeted by Ras transformation, which was initially characterized as the p28 component of the 26S proteasome, and recently identified as an oncoprotein. This was the first evidence to show that gankyrin pathway was implicated in Ras-activated transformation. Therefore, our proteomics analysis could provide more complete insight into the dissection of downstream signaling pathways of transformation by Ras.

Experimental Procedures

Plasmids, Cells, Transfection, and Reagents. Human oncogenic Ras plasmid (H-RasV12) and the control vector were gifts of Dr. J. Pedro Vaqué (Santander, Spain). NIH3T3 cell line was obtained from ATCC, maintained in Dulbecco's modified Eagle's medium (DMEM, Life Technologies) containing 10% FBS and 1% penicillin/streptomycin. NIH3T3 cells were transfected by Lipofectamine 2000 (Life Technologies, Inc.) with

* Correspondence to Xuemin Zhang, National Center of Biomedical Analysis, 27 Tai-Ping Road, Beijing 100850, China. Tel.: 86-10-66930169. Fax: (8610) 68246161. E-mail: xmzhang@nic.bmi.ac.cn. Dr. Ai-Ling Li: e-mail, lal@proteomics.cn.

§ Both authors contributed equally to this work.

10.1021/pr060283f CCC: $33.50

Published on Web 08/17/2006

pcDNA3-IRES-Luc vector containing human oncogenic H-RasV12. Stable clones were established in the presence of 600 μg/mL Geneticin (G418) and were further characterized. The antibodies of anti-BTF3 (sc-28717) and anti-gankyrin (sc-8991) were purchased from Santa Cruz Biotechnology, Inc. (Santa Cruz, CA), and anti-Ras antibody (#3965) was purchased from Cell Signaling Company.

Construction of Gankyrin Reporter Vector and Luciferase Assays. The reporter vector of mouse gankyrin was constructed by cloning a 1002 bp putative gankyrin promoter region into pGL3-Basic reporter vector (Promega), consisting of the mouse gankyrin promoter driving the firefly luciferase gene. The proximal promoter region was first amplified by PCR from the genome of NIH3T3 using primers based on the genomic DNA sequence of the mouse gankyrin gene (about 1 kb before the translation initiation site). The forward primer designed (-CCGCTCGAGAGCCCTGTTCTATACCATAACAAAGGAG-) contained the Xho I restriction enzyme site at the 5′ end, while the reverse primer designed (-CCCAAGCTTTCGCCTTCCCAAGACCTCCGTGAAACT-) carried a Hind III site. The PCR product was then cloned into the pGL3-Basic reporter vector with the same sites. In luciferase activity assay, a renilla luciferase control reporter vector pRL-TK (Promega) was cotransfected. Twenty-four h after transfection, cells were lysed and luciferase activity was assayed using the Dual-Luciferase Reporter Assay System (Promega) by a Turner Design, TD 20/20, Luminometer (Sunnyvale, CA) according to the manufacturer's recommendations.

Animal Care, Subcutaneous Injection, and Tumor Growth in Vivo Imaging. Strict animal care procedures were carried out for all experiments according to international common animal care and use guidelines. Animals used in this study were nude mice, 5−10 weeks old (National Center of Biomedical Analysis, Beijing). H-RasV12 stably expressed NIH3T3 cells and the control NIH3T3 cells (2×10^6) were implanted by subcutaneous injection into the dorsal region near the thigh of female nude mice. Tumor growth was monitored weekly for 6 weeks by caliper measurements (L × W × D) and weekly by in vivo bioluminescent imaging (BLI). The in vivo imaging was performed as described using an Imaging System (IVISTM, Xenogen).[12−14] Briefly, nude mice were given substrate D-luciferin by intraperitoneal injection at a dose of 150 mg/kg body weight (30 mg/mL of luciferin stock) prior to imaging and anesthetized with isoflurane/oxygen. Mice were then placed on the warmed imaging stage inside the light-tight camera box with continuous exposure to 1−2% isoflurane. Mice were imaged from the tergal side for 1 min or 30 s, 5 min following the injection of luciferin. Relative photon emission from regions of interest was quantified using Living Image TM software (Xenogen) as an overlay on Igor image analysis software (Wavemetrics).

Sample Preparation. To obtain total protein lysates, 80−90% of confluent cells was washed with chilled phosphate-buffered saline, and cell lysates were then prepared on ice using cool lysis buffer (8 M urea, 4% CHAPS, 40 mM Tris, 1 mM EDTA, 1 mM EGTA, 60 mM DTT) containing a protease inhibitor cocktail (Roche Diagnostic). After 30 min of gentle stirring at 4 °C, the sample was centrifuged at 12 000*g* (Eppendorf, Hamburg, Germany) for 30 min. The supernatant was collected, and protein concentration was determined using the Bradford method. Then, the lysates were aliquoted and stored at −80 °C until used.

Two-Dimensional Electrophoresis. Two-dimensional electrophoresis (2-DE) was performed as described by Görg et al.[15]

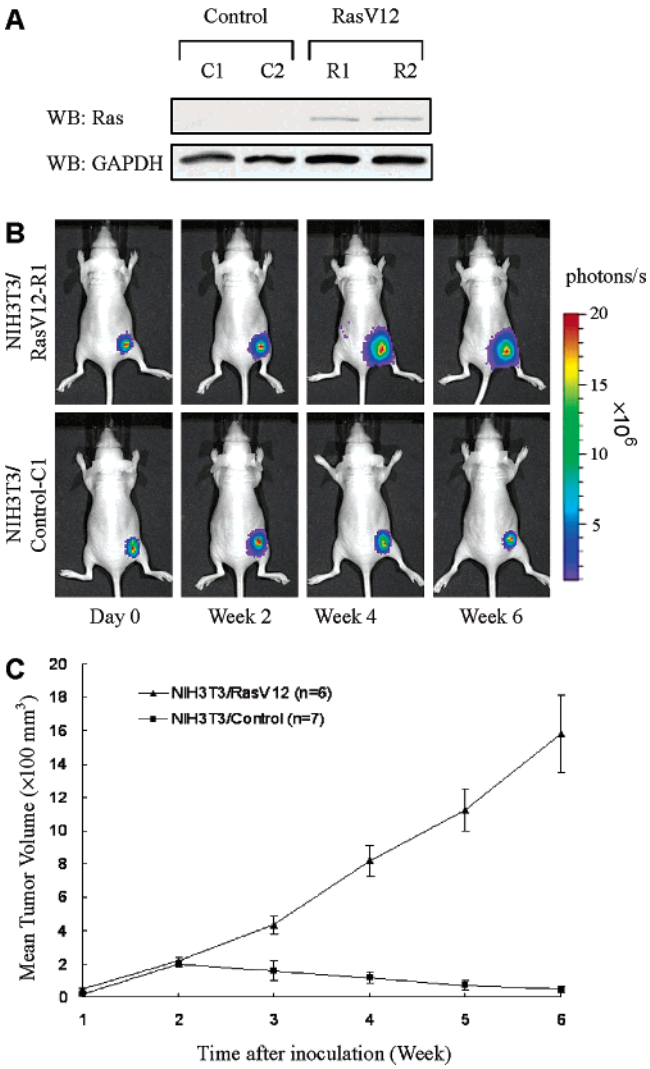

Figure 1. Oncogenic Ras could induce phenotypes of transformation on NIH3T3 cells. (A) Lysates (30 μg) from H-RasV12 stable expressed NIH3T3 cells (R1 and R2) and the control cells (C1 and C2) were collected for Western blot analysis; C1, C2, R1, and R2 indicate the different clones. (B) The H-RasV12-transformed NIH3T3 cells formed tumors subcutaneously in nude mice, and the inoculation protocol was described in detail in Experimental Procedures. Luciferase signals (photons/s) from inoculation regions of images were quantified using LivingImage software. (C) Subcutaneous tumor growth curve of Ras-transformed NIH3T3 cells. H-RasV12 stably expressed NIH3T3 cells and the control NIH3T3 cells (2×10^6) were implanted by subcutaneous injection into the dorsal region near the thigh of female nude mice. Tumor growth was monitored weekly for 6 weeks by caliper measurements (L × W × D).

Briefly, isoelectric focusing was done with the IPGphor system (Amersham Pharmacia Biotech, Uppsala, Sweden). Immobiline 3-10 linear DryStrips (Pharmacia Biotech) were rehydrated for 10 h using reswelling buffer (8 M urea, 2% CHAPS, 20 mM dithiothreitol) and IPG Buffer (0.5%). SDS-PAGE was performed using 13% polyacrylamide gels without a stacking gel in the PROTEAN II cell (Bio-Rad Co.). Following SDS-PAGE, gels were stained with 0.1% (w/v) Coomassie Blue G-250 in 50% methanol and 10% acetic acid, or silver stain according to the protocol of Shevchenko et al.,[16] and gel image analysis was processed using Adobe Photoshop software and the Diversity One program (Pharmacia).

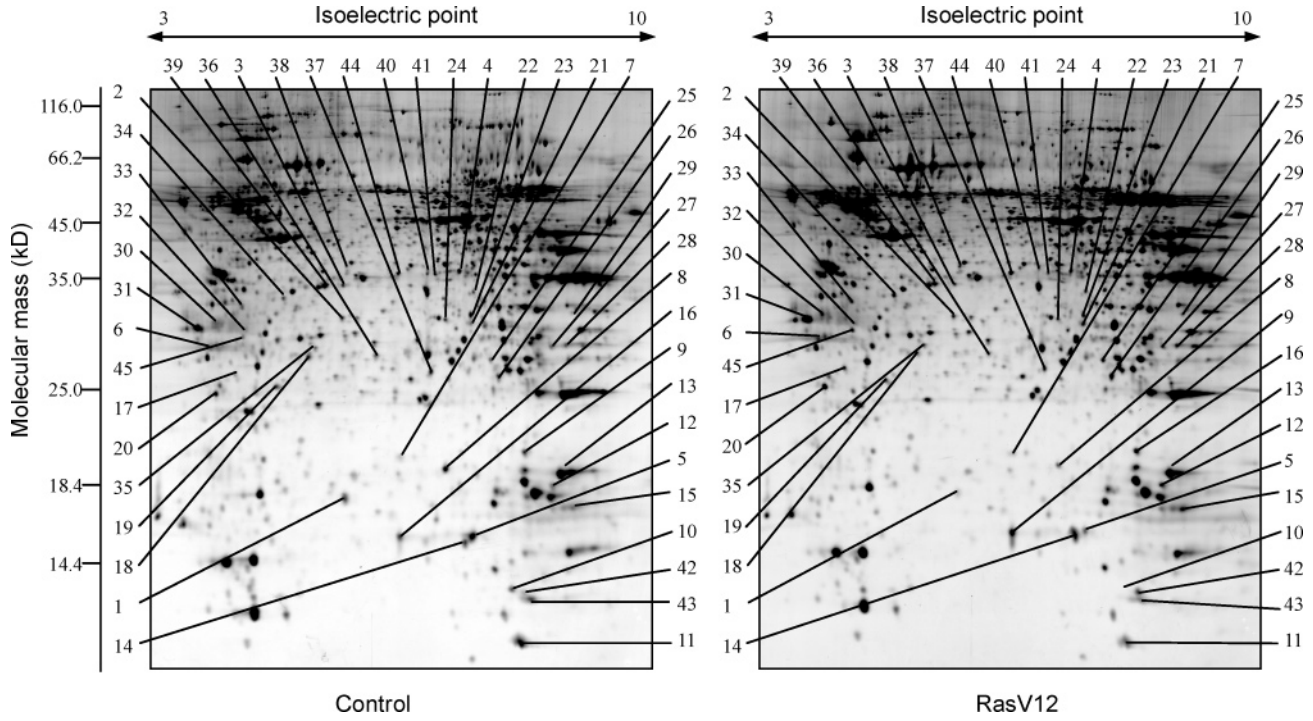

Figure 2. 2-DE analysis of differentially expressed protein spots between Ras-transformed NIH3T3 cells and the control cells. Total cell lysates (125 μg) of Ras-transformed NIH3T3 cells and the control cells were subjected to 2-DE analysis and detected by silver staining. The pH gradient of the first-dimension electrophoresis is shown on top of the gels, and migration of molecular mass markers for SDS-PAGE in the second dimension is shown on the left side. The original gel size was 20 $\times$ 20 $\times$ 0.1 cm^3. The marked protein spots were significantly altered between transformed cells and the control cells. The results of identification by mass spectrometry were listed in Table 1.

In-Gel Digestion. In-gel digestion was performed using a modified version of a previously published protocol.[17] Briefly, protein spots were excised from two-dimensional gels stained with Coomassie Blue G-250 and were destained by washing in 200 μL aliquots of 50 mM ammonium bicarbonate in 50% (v/v) acetonitrile for 30 min. The gel pieces were then dried in a SpeedVac Vacuum (Savant Instruments, Holbrook, NY) and rehydrated at 4 °C for 30 min in 10 μL digestion solution (25 mM ammonium bicarbonate and 0.01 μg/μL modified sequence-grade trypsin); 4−10 μL of digestion solution without trypsin was then added to keep the gel pieces wet during the digestion. After incubation overnight at 37 °C, the digestion was stopped with 5% TFA for 20 min. Peptides were extracted by 20 μL of 5% TFA for 1 h at 37 °C and then by 20 μL of 2.5% TFA/50% acetonitrile for 1 h at 37 °C. The combined supernatants were evaporated in the SpeedVac Vacuum and dissolved in 4 μL of 0.5% aqueous TFA for mass spectrometric analysis.

MS Analysis. All mass spectra of MALDI-TOF-MS were obtained on a Bruker REFLEX III MALDI-TOF-MS (Bruker-Franzen, Bremen, Germany) in positive ion mode at an accelerating voltage of 20 kV with the matrix of α-cyano-4-hydroxy cinnamic acid. Internal calibrations were performed using tryptic autolysis products. Peptide mass fingerprinting (PMF) data were analyzed by searching through the Swiss-Prot and NCBInr database by the Mascot search engine (http://www.matrixscience.co.uk) with a tolerance of approxiamtely ±0.3 Da, one missed cleavage site, and peptide modifications by acrylamide adducts with cysteine and methionine oxidation. Proteins identified by PMF were further evaluated by comparing the calculated and observed molecular mass and p*I*, as well as the number of peptides matched and percent sequence coverage. ESI−MS/MS experiments were performed on a Q-TOF2 mass spectrometer (Micromass, U.K.) with a nanoflow Z-spray source. Peptide sequencing was performed using palladium-coated borosilicate electrospray needle (Protana, Denmark). The mass spectrometer was operated in the positive ion mode with a source temperature at 80 °C, and a potential of 800 V applied to the Nanospray probe. The amino acid sequences of the peptides were deduced with peptide sequencing program MasSeq. The database search was finished with the Mascot search engine (http://www.matrixscience.co.uk) using the data processed through MaxEnt3 and MasSeq.

RNA Isolation and Semiquantitative RT-PCR Analysis. Total RNAs were isolated from 1 $\times$ 10^6 cells by using TRIzol Reagent (15596-026, Invitrogen) according to the manufacturer's instructions. Primers used to amplify the gene fragments were available from the authors. We used MMLV Reverse Transcriptase (M1701, Promega) for semiquantitative RT-PCR following the manufacturer's instructions. We performed PCR amplifications of 20 cycles for glyceraldehyde-3-phosphate dehydrogenase and 30 cycles for fragment of target genes.

Western Blot. Whole cell lysates (20 μg) in 1$\times$ SDS loading buffer were subjected to electrophoresis in 12% or 15% SDS-PAGE at 100 V. The gel was transferred onto 0.2 μm pore NC membrane at 40 V for 2 h. The membrane was then blocked overnight with 5% nonfat milk in TBS-Tween and probed with specific monoclonal antibody at a 1:1000 dilution for 1.5 h. After being washed, the membranes were incubated with a 1:2000-diluted HRP-conjugated secondary antibody. Antibody−antigen complexes were detected by enhanced chemiluminescence (ECL) kit according to manufacturer's instruction (Amersham Life Science).

Table 1. List of Proteins Identified by Mass Spectrometry Significantly Changed between Ras-Transformed NIH3T3 and the Control Cells[a]

spot no.	protein name	NCBI ID no.	abbr. name	M_r (kDa) theor.	M_r (kDa) obsd.	p*I* theor.	p*I* obsd.	Peptides match	Peptides total	sequence coverage (%)	MS/MS	score	protein expression	reported
1	T cell receptor beta	AAT98241	TCR β	14.936	15.545	8.55	7.08	6	23	38	N	67	↓	+
2	F-actin capping protein beta subunit	P47757	Capzb	31.214	31.252	5.47	6.05	9	16	32	N	97	↓	+
3	Capping protein muscle Z-line, alpha 2	NP_031630	Capza2	32.947	34.884	5.57	6.07	11	21	58	N	89	↓	−
4	Aminolevlinate, delta-, dehydratase	NP_032551	Alad	36.023	37.065	6.32	6.46	10	25	31	N	86	↓	−
5	Keratinocyate lipid-binding protein	CAA49703	Mal1	15.127	15.212	6.14	6.60	7	18	45	N	63	↓	−
6	40S ribosomal protein S12	NP_999528	RPS12	14.514	15.157	6.81	7.09	8	26	56	N	66	↓	−
7	Basic transcription factor 3-like 4	NP_081729	Btf3l4	17.260	16.617	5.95	6.29	6	10	24	N	65	↓	−
8	Cofilin 1, nonmuscle	NP_031713	Cfl1	18.548	19.293	8.22	7.29	7	19	35	N	68	↓	+
9	Basic transcription factor 3	AAH64010	BTF3	22.017	21.294	9.52	9.23	9	17	31	Y	89	↑	−
10	Macrophage migration inhibitory Factor	1MFIC	MIF	12.365	12.577	7.28	8.08	6	10	43	Y	71	↓	+
11	Ubiquitin	751846A	Ubq	8.446	8.436	6.56	8.19	6	9	57	Y	96	↓	+
12	Destrin	NP_062745	Dstn	18.521	18.333	8.14	8.57	8	15	35	Y	78	↑	−
13	Cofilin 1, nonmuscle	NP_031713	Cfl1	18.548	19.323	8.22	9.07	6	14	40	N	94	↓	+
14	Histidine triad nucleotide binding protein 1	NP_032274	Hint1	13.776	14.882	6.36	6.51	11	18	53	Y	143	↑	+
15	Hist1h2bc protein	AAH11440	Hist1h2bc	14.930	14.977	10.13	9.83	7	12	32	N	79	↑	−
16	Fatty acid binding protein 5	NP_034764	Fabp5	15.137	15.268	6.14	6.76	9	26	50	N	67	↑	+
17	Calcium binding protein P22	NP_062743	CHP	22.432	23.020	4.97	4.78	5	8	35	N	69	↑	−
18	Beta-actin (aa 27−375)	CAA27396	Actin	39.161	37.444	5.78	5.66	6	15	26	N	75	↓	−
19	HP1 alpha protein	CAA67960	HP1 alpha	22.172	23.000	5.71	5.28	7	17	32	N	67	↓	−
20	Tumor protein, translationally controlled 1	AAH86358	TPT1	19.450	20.453	4.76	4.55	12	19	51	Y	77	↑	+
21	Glutathione *S*-transferase omega 1	NP_034492	Gsto1	27.480	27.838	6.91	7.59	9	16	36	N	97	↑	−
22	Prps2 protein	AAH24942	Prps2	34.764	34.080	6.15	6.64	8	18	35	N	106	↓	−
23	Hypothetical protein LOC241134	AAH82310		80.129	31.671	9.10	8.60	7	14	15	N	68	↓	−
24	Carbonyl reductase 3	NP_766635	Cbr3	30.934	31.044	6.15	6.29	11	21	51	N	65	↓	−
25	Hypoxanthine−guanine phosphoribosyltransferase	Q64531	HPRT1	24.066	25.062	5.74	5.82	7	15	36	N	64	↑	−
26	Proteasome (prosome, macropain) subunit, beta type 2	AAH08265	Psmb2	22.892	22.847	6.52	6.92	5	9	41	N	65	↑	−
27	F-box and leucine-rich repeat protein 18	NP_001028484	Fbx118	77.621	28.564	8.85	8.57	6	8	21	N	64	↑	−
28	Glutathione *S*-transferase, mu 1	AAH46758	Gstml	25.953	28.659	7.72	7.73	8	23	30	Y	98	↑	−
29	ATPase, H+ transporting, V1 subunit E isoform 1	BAE26943	ATP6V1C1	26.145	31.777	8.44	8.81	7	13	39	N	68	↑	−
30	Tropomyosin 3 isoform 2	XP_890343	TPM3−2	28.991	30.532	4.77	4.53	8	13	35	Y	66	↑	+
31	Unnamed protein product	XP_901898		29.170	30.228	4.63	4.32	6	21	32	N	78	↑	−
32	Otoconin−90	NP_035083	Oc90	49.049	29.335	4.72	4.87	7	25	42	N	69	↑	−
33	Triosephosphate isomerase	CAA37420	Tpi−1	20.160	22.527	5.41	4.96	8	12	34	N	87	↑	−
34	Spermidine synthase	BAE27138	SRM	33.973	33.405	5.31	5.36	13	25	61	N	65	↑	+
35	6-phosphogluconolactonase	NP_079672	Pgls	27.237	28.280	5.55	5.75	6	13	33	N	66	↑	+
36	Phosphoserine phosphatase	NP_598661	Psph	25.080	27.628	5.81	6.46	14	27	53	N	94	↓	+
37	Proteasome beta 3 subunit	AAH14783	Psmb3	22.949	26.194	6.15	6.21	11	21	42	Y	79	↓	−
38	Alpha enolase (Enolase 1)	P17182	Eno1	46.980	47.558	6.37	6.09	9	13	24	N	89	↑	+
39	Anxa3	CAJ18488	Anxa3	36.304	34.884	5.50	5.86	12	27	49	N	160	↓	−
40	Histidine triad protein member 5	NP_081306	Dcps	38.964	36.739	6.02	6.08	11	18	36	Y	78	↓	−
41	Aryl-hydrocarbon receptor-interacting protein	AAH75614	Aip	37.581	36.578	5.97	6.18	16	31	37	N	100	↓	−
42	CPN10-like protein	AAF79149	Cpn10−rsl	10.971	12.440	8.89	8.23	12	17	34	Y	65	↑	−
43	Heat shock protein 1	AAH24385	HSP1	10.956	12.170	7.93	8.32	9	15	23	N	67	↓	+
44	Transaldolase 1	AAH04754	Taldo1	37.363	36.578	6.57	6.72	11	25	28	N	70	↑	−
45	Proteasome 26S subunit, non-ATPase, 10	NM_016883	Gankyrin	25.115	26.018	5.68	6.28	12	17	38	Y	89	↑	+

[a] The calculation of experimental p*I* and M_r was based on migration of the protein spot on 2-D gels. MS/MS indicates that the corresponding protein spot has been further identified by Q-TOF2 MS, partial sequencing analysis. ↑↓ shows the expression change trend of Ras-transformed NIH3T3 proteins compared with the control cells, ↑ means the protein expression increased in Ras-transformed cells, and ↓ means the protein decreased. "Reported" means that whether the protein has been reported to be linked to Ras-induced transformation or cancer, '+' shows that the protein has been reported to be linked to Ras-induced transformation or cancer and '−' shows none. The spot numbers correspond to those on the 2-DE images shown in Figure 2.

Results

Transformation of NIH3T3 Cells by H-RasV12. To analyze the profiling of H-RasV12 activated transformation, we transfected mouse NIH3T3 cells with plasmids coding for the neomycin-resistance gene alone (control) or with H-RasV12 gene. Stable cell transfectants were selected in the presence of G418. The Ras protein expression level in these reconstituted cells was determined by Western blot using Ras polyclonal antibodies (Figure 1A). The control and H-RasV12-transfected cells differed in morphology and colony formation capacity in

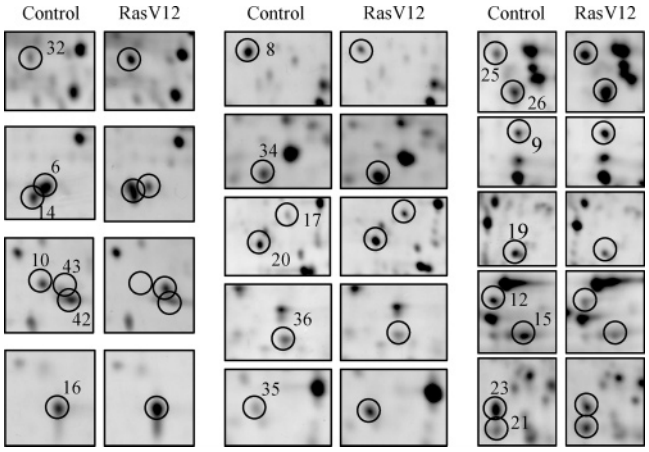

Figure 3. Close-up sections of some altered protein spots between Ras-transformed cells and the control cells. The compared sections are close-up of silver-stained 2-DE gels as shown in Figure 2, and the no. of protein spot is the same as shown in Table 1.

soft agar (data not shown). To evaluate the effects of H-RasV12 on transformation or tumorigenesis, we further established the stably transfected NIH3T3 cell lines using the H-RasV12-IRES-Luc expression vector, and detected the growth of subcutaneous tumor formation of the cell lines in vivo. As shown in Figure 1B, we injected 2×10^6 bioluminescent NIH3T3 cells into nude mice to monitor subcutaneous tumor growth. Bioluminescence of tumor growth was measured beginning on day zero and weekly thereafter and compared to external caliper measurements of the same tumor sites (Figure 1C). By week 4, all mice injected with H-RasV12-transformed NIH3T3 cells showed successful tumor development. In contrast, tumor development was not obvious in the control mice. Accurate measurement of tumor volume by the caliper method was consistent with the results by bioluminescent detection (Figure 1C).

2D Proteome Maps To Identify Proteins Involved in Ras-Mediated Transformation. Total lysates from the two cell lines of H-RasV12-transformed cells and the control cells were analyzed in five independent experiments by 2-DE. Figure 2 showed representative 2-DE images of Ras-transformed and the control cells, and we reproducibly detected more than 1000 distinct protein spots with silver staining. Landmark protein spots (such as actin and others) did not change in the two groups and were chosen to use for standardization. All of the spots marked in Figure 2 were distributed in *pI* 3∼10 and their molecular masses ranged from 10.0 to ∼116.0 kDa, which were conformed to achieve a better dynamic separation range and reproducibility.

From the gels, we noticed 45 protein spots that altered significantly in their expressions in the Ras-transformed NIH3T3 cells compared with the control cells. Among the spots marked in Figure 2, 23 proteins increased in their levels, while 22 decreased in their expression in response to Ras transformation (Table 1). The close-up section patterns of 21 altered protein spots, shown in Figure 3, clearly indicated the changes of their expressions in response to Ras transformation, whereas some other spots in the same section could be found unchanged.

The 45 protein spots selected were subjected to in-gel trypsin digestion and analysis with MALDI-TOF-MS and ESI−MS/MS. We successfully identified all of the 45 protein spots, corresponding to 44 proteins (Table 1). The analysis of PMF has been made for at least five samples from five independent experiments. The reliability of these results identified by PMF was evaluated by MOSCOW values and sequence coverage. After database searching with PMF, protein score was significant ($P < 0.05$), with a difference between measured and calculated masses below 0.3 Da. In addition, the apparent observed molecular mass and isoelectric point for all identified proteins matched very well with their calculated values. For some identifications concluded by PMF results, ESI−MS/MS were further used to sequence at least two peptides chosen from the corresponding PMF, which was consistent with the analysis by PMF (Figure 4).

Clustering of Identified Proteins. Most of these identified proteins, affected by Ras-mediated transformation, could be classified into several general groups according to their cellular functions, including signal transduction, cytoskeleton, metabolism, protein degradation, transcription, translation, and ionic homeostasis (Table 2). Among the identified proteins, a total of 16 proteins had been known to be involved in tumor or oncogenic transformation (Table 1). For example, the enhanced expression of 6-phosphogluconolactonase and phosphoserine phosphatase we found was in agreement with the previous report on Ras-induced transformation.[3] The other 28 proteins identified have not been described before to be involved in transformation. Identification of these targets suggested novel ways of Ras-mediated oncogenic transformation in regulatory network of tumor cells, and required to be further explored. The largest protein group consisted of enzymes involved in cellular metabolism. In total, 13 proteins have been identified within this category, and most of these proteins were up-regulated.

Transcriptional Level and Western Blot Analysis of Ras-Transformed Effects. Those differentially expressed proteins are commonly regulated at the transcriptional level and/or through translational and post-translational modifications. To explore the mechanisms leading to the changes of the identified proteins in response to Ras-induced transformation, we randomly selected 16 genes for semiquantitative RT-PCR analysis and two proteins for Western blot analysis. For RT-PCR analysis, total RNAs isolated from different clones of H-RasV12-transformed NIH3T3 cells and the control cells were used as templates. We found that the changes of seven genes (RPS12, MIF, Gankyrin, Fabp5, TPT1, Psmb2, and Eno1) at the mRNA levels were consistent with those at protein expression levels in the Ras-transformed NIH3T3 cells (Figures 5 and 2). Only the change of heterochromatin protein 1 (HP1) at mRNA level was inconsisitent with its protein level. The other eight genes (Mal1, BTF3, Cfl1, Hint1, Dstn, His1h2b, Psmb3, and Anax3) were not found to have changed significantly in their transcriptional levels. Western blot results showed that alterations in expression level of two transformation-related proteins selected, including basic transcription factor 3 (BTF3) and gankyrin in NIH3T3 cells oncogenically transformed by Ras, were consistent with our 2-DE gel analysis (Figure 6A). The exact function and mechnism remain to be further investigated.

An interesting finding in our study was the up-regulation of gankyrin, a recently found oncoprotein, in Ras-transformed cells. Semiquantitative RT-PCR and Western blot analysis showed that gankyrin expression could be up-regulated at both transcriptional and protein levels (Figure 6A,B). To further investigate the up-regulation of gankyrin in Ras transformation cells, we constructed the reporter vector of gankyrin, consisting of the putative gankyrin promoter driving the firefly luciferase gene, and detected the relative luciferase activity in Ras-

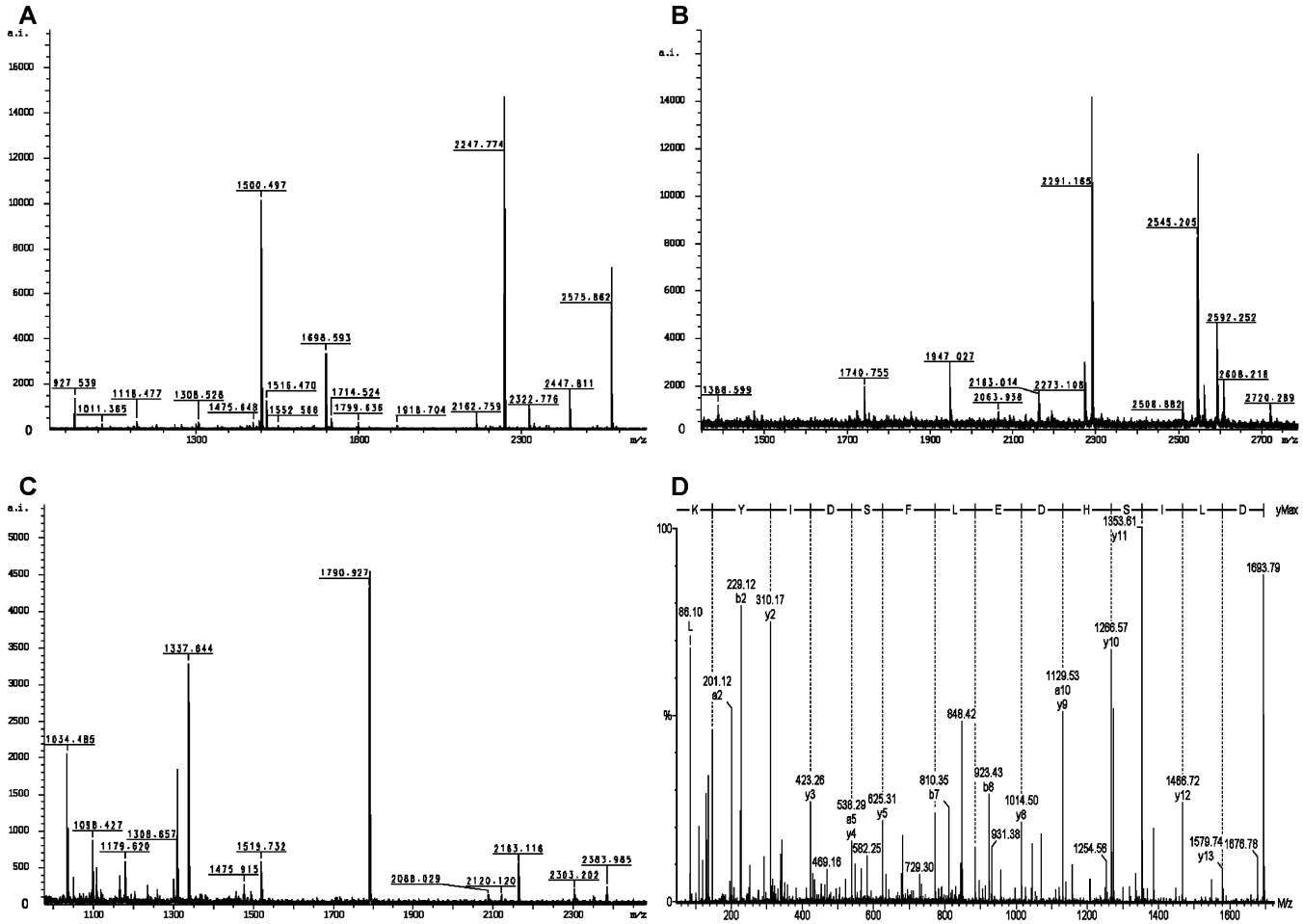

Figure 4. Identification of some differentially expressed protein spots by MALDI-TOF-MS and ESI−MS/MS. PMF identifications of Fabp5 (A), Hint1 (B), and Cfl1 (C). After database searching, protein score is significant ($P < 0.05$). (D) The peptide of 1693.79 chosen from the PMF for TPT1 was sequenced by nanoESI−MS/MS.

transformed NIH3T3 cells and the control cells. The results showed that the relative luciferase activities in Ras-transformed NIH3T3 cells were significantly higher than those in the control cells (Figure 6C), which also demonstrated the up-regulation of gankyrin at transcriptional level.

Discussion

Although Ras plays an important role in tumorigenesis, the molecular mechanism of Ras-mediated oncogenic transformation as a whole remains still obscure. With the use of a genetically defined cancer transformation mode, the dissection of downstream signaling pathways in response to Ras-mediated oncogenic transformation allows an elucidation to the mechanism. In this study, we implemented a proteomics approach to the systematical analysis on the alterations in the cellular proteome of NIH3T3 cells transformed by H-Ras, enabling the identification of numerous changes in protein expression as well as possible post-translational processing. In total, 44 proteins associated with Ras-mediated transformation have been identified by the approaches of MALDI-TOF-MS and ESI−MS/MS. Among them, 16 proteins had been individually revealed to be involved in the transformation or tumorigenesis, whereas 28 proteins were unknown before. With RT-PCR analysis, about 44% of 16 target proteins identified by the proteomics approach in this study showed concomitant changes in mRNA abundance. This was underscored by the fact that some protein expressions were not amenable to their transcriptional levels.

The protein identifications in our 2-DE proteomics screen suggested that multiple cellular processes were involved in H-Ras transformation, including metabolism, signal transduction, cytoskeleton, protein degradation, transcription, translation, and ionic homeostasis (Table 2); 30% of proteins identified involved in metabolic processes. This was not surprising since tumor cells often require higher metabolic levels to maintain a growth advantage over normal cells and was consistent with the notion of increased energy demands in cancer cells, which was consistent with the report by Young.[3] Among the identified proteins involved in metabolic processes, 6-phosphogluconolactonase and phosphoserine phosphatase were also reported to be involved in H-Ras transformation by Young. However, there were some proteins identified in each functional group which were different from those reported by Young. These were probably caused by different types of cell models used, and it implied that Ras might use different targets in different types of cells. Several of these metabolic proteins, including spermidine synthase, 6-phosphogluconolactonase, and fatty acid binding protein 5, were previously implicated in tumor formation. Interestingly, spermidine synthase was a key enzyme for post-modification of eIF-5A protein, which was revealed by the recent studies of ours and others to be involved in cell proliferation and differentiation of leukemia or lung adeno-

Table 2. Functional Classification of the Proteins Significantly Changed between Ras-Transformed NIH3T3 and the Control Cells

functional group	protein ID	function
Signal transduction	Psph	Responsible for the third and last step in L-serine formation
Signal transduction	TPT1	Implicated in cell growth, acute allergic response, and apoptosis
Signal transduction	Hint1	A haplo-insufficient tumor suppressor in mice
Signal transduction	CHP	Involved in cell communication and signal transduction
Signal transduction	Cfl1	Control morphological changes of cells by the regulation of the actin cytoskeleton
Signal transduction	Destrin	Promote rapid F-actin depolymerization in mammalian nonmuscle cells
Signal transduction	Gankyrin	A component of the 26S proteasome, and also a dual-purpose negative regulator of RB and p53
Signal transduction	MIF	Role for the mediator in regulating the function of macrophage in host defense, also acts as a phenylpyruvate tautomerase
Transcription/translation	HP1	Heterochromatin-associated protein, chromatin binding and RNA binding
Transcription/translation	Hist1h2bc	Human and mouse replication-dependent histone
Transcription/translation	BTF3	Form a stable complex with RNA polymerase II. Required for the initiation of transcription
Transcription/translation	Btf3l4	Can form a stable complex with RNA polymerase II, required for the initiation of transcription
Transcription/translation	RPS12	Involved in protein synthesis
Transcription/translation	Ubq	In DNA repair and the activation of protein kinases such as IkappaB kinase
Ionic homeostasis	ATP6V1C1	Mediates acidification of eukaryotic intracellular organelles
Ionic homeostasis	Prps2	An essential cofactor which supports the physiological activity of sodium−potassium exchangers (NHEs) family members
Protein degradation	Psmb2	Member of proteasome B-type family, also known as the T1B family, that is a 20S core beta subunit
Protein degradation	Ubq	Best known for its function in targeting proteins for degradation by the proteasome
Protein degradation	Psmb3	Member of proteasome B-type family, also known as the T1B family, that is a 20S core beta subunit
Metabolism	Pgls	Hydrolysis of 6-phosphogluconolactone to 6- phosphogluconate
Metabolism	HPRT1	Nucleotide synthesis, belongs to the purine/pyrimidine phosphoribosyltransferase family
Metabolism	Cbr3	Catalyzes the reduction of biologically and pharmacologically active carbonyl compounds to their corresponding alcohols
Metabolism	Prps2	Belongs to the ribose-phosphate pyrophosphokinase family
Metabolism	Gsto1	Exhibits glutathione-dependent thiol transferase and dehydroascorbate reductase activities
Metabolism	Fabp5	Modulates adipose tissue function and contributes to systemic glucose metabolism
Metabolism	Gstml	Glutathione transferase activity
Metabolism	SRM	Conversion of putrescine to spermidine using decarboxylated S-adenosylmethionine as the cofactor
Metabolism	ANXA3	Diphosphoinositol-polyphosphate diphosphatase activity
Metabolism	Taldo1	A key enzyme of the nonoxidative pentose phosphate pathway
Metabolism	Alad	Catalyze the second step of heme synthesis
Metabolism	Mal1	Modulate adipose tissue function and contributes to systemic glucose metabolism
Metabolism	Tpi-1	Enzyme for glycolysis, reversibly catalyzes the isomerization of D-glyceraldehyde 3-phosphate to dihydroxyacetone phosphate
Structural proteins	TPM3-2	Actin-binding protein, can stabilize microfilaments
Structural proteins	Actin	One of the two nonmuscle cytoskeletal actins, involved in cell motility, structure and integrity
Structural proteins	Capzb	Actin modification
Structural proteins	Capza2	Actin modification
Structural proteins	Oc90	Major extracellular matrix protein

carcinomas.[18,19] Notably, 46% of the metabolic proteins identified in this study were phosphokinases and phosphases, which were possibly involved in increased metabolisms. We also noticed that, among these identified targets, one notable subgroup consisted of several enzymes, including glutathione *S*-transferase mu 1, aminolevlinate dehydratase, glutathione *S*-transferase omega 1, triosephosphate isomerase, transaldolase 1, and keratinocyate lipid-binding protein, which were involved in cellular redox balance. Cellular redox balance was also reported by Young to be involved in Ras transformation.[20] This suggested that Ras transformation increased the overall antioxidant capacity of cells.

Several of the identified protein targets, including proteasome subunit beta type 2, proteasome subunit beta 3, proteasome 26S subunit non-ATPase 10, and ubiquitin, were components of the ubiquitin-proteasome (UP) system. The UP system is essential to many physiological and fundamental cellular processes, and the abnormal activity of the system is known to be implicated in tumorigenesis.[21] Our study showed that the system was obviously affected by oncogenic Ras-activated transformation and was possibly associated with cancer development and Ras signaling. Moreover, it was reasonable to deduce that the alterations of the systems should be accompanied by series changes of many signal pathways, since the UP system is a well-characterized pathway that is involved in regulating nearly every cellular process that occurs in eukaryotes. Consistently, the changes revealed by our studies included components of pathways of apoptosis, DNA repair, transcription regulation, and ionic homeostasis.

An interesting finding in our study was the up-regulation of gankyrin, a recently found oncoprotein,[22−25] in Ras-transformed cells. Gankyrin was initially purified and characterized by Tanaka and co-workers as the p28 component of the 19S regulatory subunit of the 26S proteasome. Recently, Fujita and colleagues identified gankyrin as a gene that was consistently overexpressed in human liver cancers.[22−25] Gankyrin binds cyclin-dependent kinase 4 (CDK4), competing with p16INK4A, an inhibitor of cyclin kinases, for binding to CDK4. Thus, by inhibiting p16INK4A, gankyrin accelerates phosphorylation and proteasomal degradation of RB, enhancement of E2F1-mediated transcription, and cell cycle progression.[23] Gankyrin also binds to MDM2, facilitating p53-MDM2 binding, and increases ubiquitylation and degradation of p53.[24] However, there is no indication so far that gankyrin pathway is implicated in Ras-activated transformation. In this study, we found that gankyrin was up-regulated at both mRNA and protein levels in response

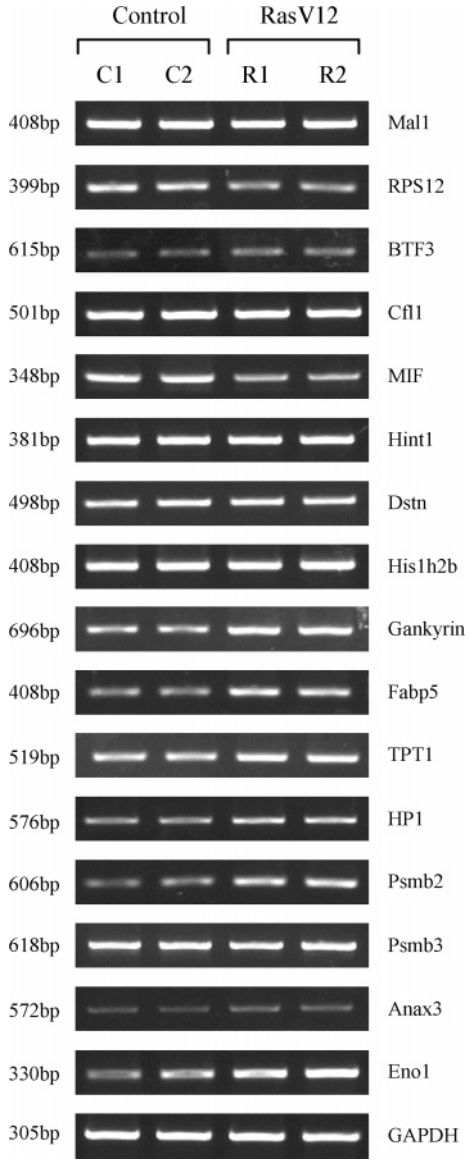

Figure 5. Analysis of the differentially expressed protein spots between Ras-transformed cells and the control cells. The length of each amplified fragment is marked on the left and the name of the gene on the right. The mRNA expression levels of 16 differentially expressed proteins in 2-DE gels were analyzed by RT-PCR. C1 and C2 were different control clones; R1 and R2 were different Ras-transformed NIH3T3 clones. GAPDH was used as an internal control.

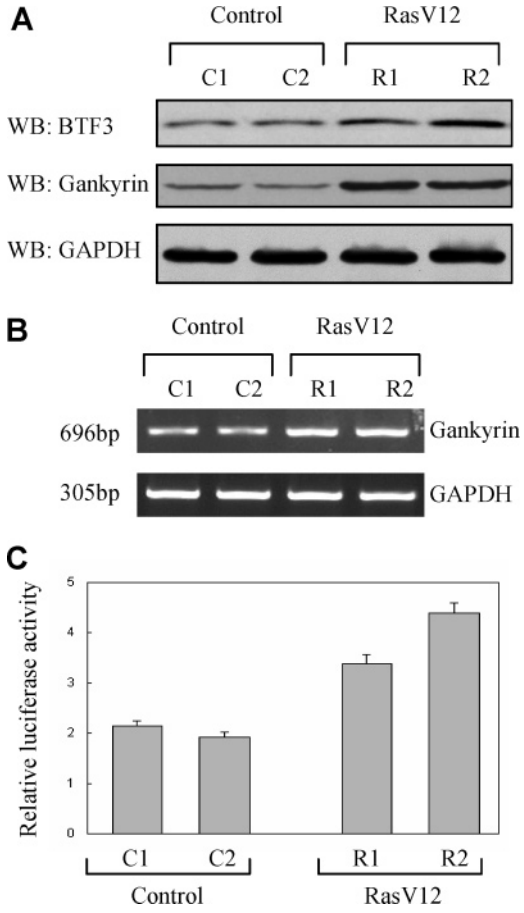

Figure 6. Analysis of the alternations of gankyrin and BTF3. (A) Up-regulation of gankyrin and BTF3 was detected by Western blot analysis in Ras-transformed cells and the control cells. (B) Up-regulation of gankyrin at mRNA level was detected by RT-PCR analysis. (C) Up-regulation of gankyrin at transcriptional level was further detected by reporter assay. C1 and C2 were different control clones; R1 and R2 were different Ras-transformed NIH3T3 clones. GAPDH was used as an internal control.

to Ras-mediated transformation. With regards to the importance of gankyrin in the regulation of oncogenic transformation and that its overexpression contributes to tumorigenesis, our findings raised the possibility that gankyrin up-regulation was a downstream signal of Ras transformation. Biologically, it required to be further demonstrated that gankyrin pathway plays a pivotal role in Ras transformation.

Another finding in our study was the down-regulation of HP1, which also interacts with RB, and is essential for inhibition of gene transcription by RB/E2F repressor complex.[26] HP1 overexpression leads to an increase in gene silencing, and gene expression appears to be sensitive to HP1 dosage.[27,28] We theorized that down-regulation of HP1 in Ras-transformed cells might partially eliminate the inhibition of many genes, which could contribute to the significant changes of phenotype and the up-regulation of some proteins identified in this study. It has not been reported so far that HP1 was regulated in Ras transformation, and the exact mechanism that the HP1 pathway exerts in Ras transformation remains to be further determined.

Taken together, we implemented a proteomics approach to the systematical analysis of the alterations in the cellular proteome of NIH3T3 cells transformed by H-Ras. In total, 44 proteins associated with Ras-mediated transformation have been identified, including 28 proteins previously unknown to be implicated in the processes. Interestingly, several of the identified protein targets were components of the UP system, indicating the UP system was obviously affected by Ras-activated transformation. Moreover, a principal finding in our study was the up-regulation of gankyrin in Ras-transformed cells. This was the first evidence to show that oncoprotein gankyrin was implicated in Ras-activated transformation. Therefore, our proteomics analysis provided more complete insight into the dissection of downstream signaling pathways of transformation by Ras.

Abbreviations: 2-DE, two-dimensional electrophoresis; UP, ubiquitin-proteasome; BTF3, basic transcription factor 3; PMF,

peptide mass fingerprinting; BLI, bioluminescent imaging; CDK4, cyclin-dependent kinase 4; HP1, heterochromatin protein 1.

Acknowledgment. We thank Dr. J. Pedro Vaqué for providing various constructs of Ras. This work was supported by the National Natural Science Foundation of China (30500583, 30525021, and 30321003), and granted from National 973 Project (2006CB500700).

References

(1) Kato, K.; Horiuchi, S.; Takahashi, A.; Ueoka, Y.; Arima, T.; Matsuda, T.; Kato, H.; Nishida, J. J.; Nakabeppu, Y.; Wake, N. *J. Biol. Chem*. **2002**, *277*, 11217−11224.
(2) Stewart, S.; Guan, K. L. *J. Biol. Chem*. **2000**, *275*, 8854−8862.
(3) Young, T.; Mei, F.; Liu, J.; Bast, R. C.; Kurosky, A.; Cheng, X. *Oncogene* **2005**, *24*, 6174−6184.
(4) Ma, P. H.; Magut, M.; Chen, X. B.; Chen C. Y. *Mol. Cell. Biol.* **2002**, *22*, 2928−2938.
(5) Adams, J. M.; Cory, S. *Science* **1991**, *254*, 1161−1167.
(6) Tuveson, D. A.; Jacks, T. *Oncogene* **1999**, *18*, 5318−5324.
(7) Mitin, N.; Rossman, K. L.; Der, C. J. *Curr. Biol.* **2005**, *15*, 563−574.
(8) Khosravi-Far, R.; White, M. A.; Westwick, J. K.; Solski, P. A.; Chrzanowska-Wodnicka, M.; Van Aelst, L.; Wigler, M. H.; Der, C. J. *Mol. Cell. Biol.* **1996**, *16*, 3923−3933.
(9) DeGregori, J. *Mol. Cell. Biol.* **2006**, *26*, 1165−1169.
(10) Liu, J.; Yang, G.; Thompson-Lanza, J. A.; Glassman, A.; Hayes, K.; Patterson, A.; Marquez, R. T.; Auersperg, N.; Yu, Y.; Hahn, W. C.; Mills, G. B.; Bast, R. C., Jr. *Cancer Res.* **2004**, *64*, 1655−1663.
(11) Anderson, N. L.; Anderson, N. G. *Electrophoresis* **1998**, 19, 1853−1863.
(12) Jenkins, D. E.; Oei, Y.; Hornig, Y. S.; Yu, S. F.; Dusich, J.; Purchio, T.; Contag, P. R. *Clin. Exp. Metastasis* **2003**, *20*, 733−744.
(13) Laxman, B.; Hall, D. E.; Bhojani, M. S.; Hamstra, D. A.; Chenevert, T. L.; Ross, B. D.; Rehemtulla, A. *Proc. Natl. Acad. Sci. U.S.A.* **2002**, *99*, 16551−16555.
(14) Zhang, N.; Weber, A., Li, B.; Lyons, R.; Contag, P. R.; Purchio, A. F.; West, D. B. *J. Immunol.* **2003**, *170*, 6307−6319.
(15) Gorg, A.; Postel, W.; Gunther, S. *Electrophoresis* **1988**, *9*, 531−546.
(16) Shevchenko, A.; Wilm, M.; Vorm, O.; Mann, M. *Anal. Chem.* **1996**, *68*, 850−858.
(17) Gamble, S. C.; Dunn, M. J.; Wheeler, C. H.; Joiner, M. C.; Adu-Poku, A.; Arrand, J. E. *Cancer Res.* **2000**, *60*, 2146−2151.
(18) Jin, B. F.; He, K.; Wang, H. X.; Wang, J.; Zhou, T.; Lan, Y.; Hu, M. R.; Wei, K. H.; Yang, S. C.; Shen, B. F.; Zhang, X. *Oncogene* **2003**, *22*, 4819−4830.
(19) Chen, G.; Gharib, T. G.; Thomas, D. G.; Huang, C. C.; Misek, D. E.; Kuick, R. D.; Giordano, T. J.; Iannettoni, M. D.; Orringer, M. B.; Hanash, S. M.; Beer, D. G. *Proteomics* **2003**, *3*, 496−504.
(20) Young, T.; Mei, F.; Yang, G.; Thompson-Lanza, J.; Liu, J.; Cheng, X. *Cancer Res.* **2004**, *64*, 4577−4584.
(21) Fuchs, S. Y. *Cancer Biol. Ther.* **2002**, *1*, 337−341.
(22) Dawson, S.; Higashitsuji, H.; Wilkinson, A. J.; Fujita, J.; Mayer, R. J. *Trends Cell Biol.* **2006**, *16*, 229−233.
(23) Higashitsuji, H.; Liu, Y.; Mayer, R. J.; Fujita, J. *Cell Cycle* **2005**, *4*, 1335−1337.
(24) Higashitsuji, H.; Higashitsuji, H.; Itoh, K.; Sakurai, T.; Nagao, T.; Sumitomo, Y.; Masuda, T.; Dawson, S.; Shimada, Y.; Mayer, R. J.; Fujita, J. *Cancer Cell* **2005**, *8*, 75−87.
(25) Higashitsuji, H.; Itoh, K.; Nagao, T.; Dawson, S.; Nonoguchi, K.; Kido, T.; Mayer, R. J.; Arii, S.; Fujita, J. *Nat. Med.* **2000**, *6*, 96−99.
(26) Young, A. P.; Longmore, G. D. *Oncogene* **2004**, *23*, 814−823.
(27) Kirschmann, D. A.; Lininger, R. A.; Gardner, L. M.; Seftor, E. A.; Odero, V. A.; Ainsztein, A. M.; Earnshaw, W. C.; Wallrath, L. L.; Hendrix, M. J. *Cancer Res.* **2000**, *60*, 3359−3363.
(28) Oliva, J.; Messaoudi, S. E.; Pellestor, F.; Fuentes, M.; Georget, V.; Balaguer, P.; Cavailles, V.; Vignon, F.; Badia, E. *FEBS Lett.* **2005**, *579*, 4278−4286.

PR060283F